Association for Information and Image Management
1100 Wayne Avenue, Suite 1100
Silver Spring, Maryland 20910
301/587-8202

Centimeter

Inches

MANUFACTURED TO AIIM STANDARDS
BY APPLIED IMAGE, INC.

1 of 1

Core Fueling to Produce Peaked Density Profiles in Large Tokamaks

D. R. Mikkelsen, K. M. McGuire, G. L. Schmidt, S. J. Zweben
Princeton Plasma Physics Laboratory
P.O. Box 451, Princeton, NJ 08543

S. E. Attenberger, W. A. Houlberg, S. L. Milora
Oak Ridge National Laboratory
P.O. Box 2009, Oak Ridge, TN 37831-8070

Abstract Peaking the density profile increases the usable bootstrap current and the average fusion power density; this could reduce the current drive power and increase the net output of power producing tokamaks. The use of neutral beams and pellet injection to produce peaked density profiles is assessed. We show that with radially 'hollow' diffusivity profiles (and no particle pinch) moderately peaked density profiles can be produced by particle source profiles which are peaked off-axis. The fueling penetration requirements can therefore be relaxed and this greatly improves the feasibility of generating peaked density profiles in large tokamaks. In particular, neutral beam fueling does not require MeV particle energy. Even with beam voltages of ~200 keV, however, exceptionally good particle confinement, $\tau_p \gg \tau_E$, is required to achieve net electrical power generation. In system with no power production requirement (e.g., neutron sources) neutral beam fueling should be capable of producing peaked density profiles in devices as large as ITER. Fueling systems with low energy cost per particle — such as cryogenic pellet injection — must be used in power producing tokamaks when $\tau_p \sim \tau_E$. Simulations with pellet injection speeds of 7 km/sec show the peaking factor, $n_{eo}/\langle n_e \rangle$, approaching 2.

1. Introduction

It has long been recognized that peaking the density profile — at fixed $\langle\beta\rangle$ and B_{tor}— increases the average fusion power density[1], and has a beneficial effect on reactor performance[2,3] which is similar to raising the β limit. The magnitude of the effect is illustrated in Fig. 1 using the peaked density profile of a supershot[4] and a flat H-mode density profile[5]. The 'extra' power could be used to run the system which produces the peaked density and will also reduce the auxiliary heating power needed for startup.

The weak temperature dependence of the fusion power near its maximum can be exploited by trading plasma density for temperature according to the needs of the fueling method: lower density facilitates neutral beam fueling, while deep pellet fueling is easier at lower temperature. A similar strategy has been used before for other purposes: the low density/high temperature regime is favorable for non-inductive

MASTER
DISTRIBUTION OF THIS DOCUMENT IS UNLIMITED

current drive (higher temperature is also associated with improved confinement in supershots[6]).

Raising the density peakedness is theoretically expected to increase the total bootstrap current and improve the current profile 'alignment', *i.e.*, the bootstrap current density is closer to the desired current density[7]. These effects lower the auxiliary current drive power and the recirculated electrical power. In addition, peaked density profiles may cause sawtooth suppression[8] which, in turn, would have beneficial consequences in large tokamaks[9–11], not the least of which is that it facilitates the creation of peaked density profiles.

It has recently been shown in detailed calculations with TPX parameters that a moderately peaked density profile is desirable for producing an 'advanced' plasma regime with reversed magnetic shear which has excellent MHD stability properties, very high bootstrap fraction, and very good current alignment[12]. Further peaking of the density profile would raise the stability threshold (for both β_N^* and β_N) of high-n ballooning modes and low-n external kink modes, but it would also drive excess bootstrap current deep in the plasma core and create a need for anti-current drive in order to maintain the negative magnetic shear that is crucial to the stability of this regime[13].

While we shall examine the use of deep fueling for the purpose of producing peaked density profiles, it should be noted that deep fueling is beneficial in several other respects. Simulations of ITER show that even relatively shallow pellet injection is preferable to gas puffing because the higher fueling efficiency (more of the particles reach the main plasma) reduces the pumping requirement and will tend to reduce the tritium inventory in the gas processing system[14]. If the D:T mix is 'tailored' by using a deep fueling method preferentially for tritium and using deuterium gas puffing it should be possible to lower the tritium concentration in the scrapeoff region and hence reduce the tritium inventory in the plasma facing components (which will become saturated with the D:T mix which flows to them).

Tokamak experiments with centrally fueled plasmas have shown that peaked density profiles often have enhanced performance. Peakedness does not uniquely determine the degree of enhanced confinement, however, and a better understanding of the causes of the enhanced confinement is desirable. High density peakedness, $n_{eo}/\langle n_e \rangle =$ 2–3, is correlated with improved energy confinement, $\tau_E/\tau_{E,L} = 2.5$–3.0, in TFTR supershots[15], as well as in high β_{pol} discharges in JT-60[16], TFTR[17,18], and DIII-D[19]. It is also associated with enhanced energy confinement in pellet fueled regimes in TFTR[20], the PEP mode in JET[21–23], and low $q(a)$ discharges in JT-60[24]. High density peakedness also occurs in high bootstrap fraction discharges in TFTR[25] and JT-60[26]. Peaked density profiles in advanced large tokamaks could facilitate access to these enhanced performance regimes.

In discharges with very good core particle confinement peaked density profiles could be maintained even if the central particle source rate is modest. All that is required is that the source be sufficient to meet the losses, so peaking of the density does not necessarily require a centrally peaked source. Indeed, density peaking has been reported during IBW heating with no beam or pellet fueling[27]. It is also important to recall that a particle 'pinch' could assist any core fueling method. In

principle, a pinch could suffice to produce a peaked density with no core particle source whatsoever; a better understanding of core particle confinement might even lead to the benefits of peaked density profiles without the costs of deep fueling systems. In the absence of such an understanding, however, we use general characterizations of transport to estimate the neutral beam and pellet injector requirements for producing peaked density profiles in power producing tokamaks.

We find that neutral beams of ~200 keV particles can fuel the core of a large tokamak but the energy cost per particle places strong constraints on the particle confinement: net electrical power can be generated only if $\tau_p \gg \tau_E$. If $\tau_p \sim \tau_E$ the fueling must be done with a system which has a lower energy per particle. Cryogenic pellet injectors have appropriate characteristics and have received considerable attention. Previous simulations of core pellet fueling in ITER produced modest peaking, $n_{eo}/\langle n_e \rangle \sim 1.1$–$1.4$, because they used relatively small, slow pellets which did not penetrate deeply[14]. We have extended that work to faster, larger pellets which lead to $n_{eo}/\langle n_e \rangle \sim 2$.

Although we will not consider it in detail, another potentially suitable fueling method is compact toroid injection[28,29]. Unlike neutral beam or pellet fueling, penetration does not depend on the tokamak plasma density or temperature and essentially all the injected mass is deposited in a small region where the toroid stops. The penetration criterion is that the initial kinetic energy density be equal to the tokamak's magnetic energy density at the deposition point. In order to keep the energy per particle low it is important to use relatively slow high-density compact toroids (high speed, low-density toroids will have a larger energy per particle). Further development is required to raise the density of hydrogenic toroids, to reduce the impurity content, and to test the penetration in ~5 T fields.

2. Core fueling by neutral beam injection

A critical design issue for the beam fueling option is the choice of beam particle energy: lower voltage minimizes the recirculating power, while higher voltage provides better penetration to the plasma core and increases the beam driven current. The inherent conflict in choosing the beam voltage is reduced by operating at low density (and consequently higher temperature), by minimizing the distance between the magnetic axis and the outboard edge of the plasma, and by maximizing the bootstrap current to reduce any required beam driven current. This permits the use of lower beam voltage and more perpendicular beam injection to enhance penetration. An optimized design thus has a higher aspect ratio, higher β_{pol}, larger Shafranov shift, higher bootstrap fraction, and, potentially, a lower current drive requirement than conventional designs. These characteristics fit naturally with the other advantages of high aspect ratio designs[30] and are also attractive for a long pulse tokamak with predominantly inductive and bootstrap current drive. Any advances in tokamak performance which lead to smaller practical reactors should also be favorable for core fueling by beams.

The first important requirement of a beam fueled system can be derived from the

equation for the net electrical power:

$$P_{\mathrm{e,net}} = \eta_{\mathrm{th}} P_{\mathrm{f}} - P_{\mathrm{b}}/\eta_{\mathrm{b}} = \eta_{\mathrm{th}} P_{\mathrm{f}} \left(1 - 1/\eta_{\mathrm{th}}\eta_{\mathrm{b}} Q\right)$$

where η_{th} is the thermal to electric efficiency of the generating system, and η_{b} is the electrical efficiency of the beam system. If the fraction of the gross electrical power which is recirculated to run the fueling beams is to be limited to a modest fraction, say 1/3, we require $Q > 3/\eta_{\mathrm{th}}\eta_{\mathrm{b}} \sim 12$, for $\eta_{\mathrm{th}} = 0.40$ [31,32] and $\eta_{\mathrm{b}} = 0.60$ for a negative-ion-based neutral beam system[33]. Lower Q would be acceptable, however, in a facility which does not produce net electrical power, e.g., a neutron source or pilot plant[34–36]. This matter is discussed in more detail — and with very similar conclusions — by Conn and Kesner[37] and their Ref. [24].

2.1. 0-d Model for Beam Fueled Plasmas

The fundamental issues of particle and energy balance in the plasma itself are readily illustrated by a 'zero-dimensional' model of a beam fueled fusion system, and a number of important qualitative conclusions can be drawn from this model. We assume a plasma of uniform density and temperature. We make no estimate of the beam penetration to the plasma core, rather, we assume all beam particles are deposited in the plasma core. This is not a valid assumption but the results of this model provide a good framework for understanding the results of the next section where beam deposition is treated realistically. An interesting complementary analysis of beam driven reactors focused on energy balance (particle fueling was not addressed) can be found in Ref. [37].

We assume equal D and T densities, $n_{\mathrm{T}} = n_{\mathrm{D}}$, and particle source rates, $S_{\mathrm{T}} = S_{\mathrm{D}}$; to provide equal beam penetration we require $E_{\mathrm{T}} = 1.5E_{\mathrm{D}}$. The fueling rate must be sufficient to maintain the density in the face of particle losses determined by the particle confinement time, $\tau_{\mathrm{D}}=\tau_{\mathrm{T}}$, and by the fusion rate:

$$S_{\mathrm{D}} = n_{\mathrm{D}}/\tau_{\mathrm{D}} + S_{\alpha}.$$

As shown above only high Q conditions are of interest so beam-target and beam-beam reactions (with $Q \leq 1$) are ignored and the fusion power density is taken to be

$$P_{\mathrm{f}} = 5E_{\alpha}S_{\alpha} = 5E_{\alpha}n_{\mathrm{D}}n_{\mathrm{T}}\langle\sigma v\rangle_{\mathrm{th}} = 5E_{\alpha}n_{\mathrm{D}}^2\langle\sigma v\rangle_{\mathrm{th}}.$$

The ratio of the fusion and beam power densities is then

$$Q = \frac{5E_{\alpha}S_{\alpha}}{5E_{\mathrm{D}}S_{\mathrm{D}}/2} = \frac{2E_{\alpha}}{E_{\mathrm{D}}}\left(\frac{n_{\mathrm{D}}\tau_{\mathrm{D}}\langle\sigma v\rangle_{\mathrm{th}}}{1 + n_{\mathrm{D}}\tau_{\mathrm{D}}\langle\sigma v\rangle_{\mathrm{th}}}\right).$$

As the particle confinement time, τ_{D} , improves Q asymptotically approaches an upper limit set by the ratio of the fusion energy release and the energy 'cost' of the beam injected pair of DT fuel ions:

$$Q_{\mathrm{limit}} = 2E_{\alpha}/E_{\mathrm{D}}.$$

While MeV beams may seem desirable since they can penetrate to the core of a large dense plasma, they cannot be used as the major fueling source in power producing tokamaks because the resulting low Q necessitates an unacceptable reduction in the net electrical power. Conversely, very low beam energy is ruled out because it leads to edge fueling and a flat density profile.

The confinement parameter required for $Q = Q_{\rm limit}/2$ is $n_{\rm D}\tau_{\rm D} = 1/\langle\sigma v\rangle_{\rm th}$. The analogous parameter for standard ignition where losses are balanced entirely by alpha heating is,

$$n_{\rm D}\tau_{\rm E}^{\rm ig} = 1.5T(n_{\rm e} + n_{\rm D} + n_{\rm T} + n_{\rm He})/E_\alpha n_{\rm D}\langle\sigma v\rangle_{\rm th} \sim 6T/E_\alpha\langle\sigma v\rangle_{\rm th},$$

and thus

$$\tau_{\rm D} \sim (E_\alpha/6T)\tau_{\rm E}^{\rm ig} \sim 60\tau_{\rm E}^{\rm ig}.$$

Thus, the particle confinement for a high performance beam fueled plasma must be much better than the energy confinement; this is particularly true for $Q > Q_{\rm limit}/2$ where Q approaches its limit asymptotically.

This requirement for very good fuel particle confinement requires us to evaluate the helium 'ash' buildup, the consequent dilution of the reacting fuel, and the reduction of the fusion power density (subjects of concern for conventional tokamaks also[38]). Taking the particle confinement time of the helium to be $\tau_{\rm He} \equiv n_{\rm He}/S_\alpha$, the ratio of the ash to deuterium density is

$$\frac{n_{\rm He}}{n_{\rm D}} = \frac{\tau_{\rm He}S_\alpha}{\tau_{\rm D}(S_{\rm D} - S_\alpha)} = \frac{\tau_{\rm He}}{\tau_{\rm D}}\left(\frac{QE_{\rm D}/2E_\alpha}{1 - QE_{\rm D}/2E_\alpha}\right).$$

Avoiding serious dilution for $Q \geq Q_{\rm limit}/2$ requires $\tau_{\rm He}/\tau_{\rm D} \ll 1$, i.e., helium confinement must be much less than that of the fuel ions (Fig. 2a).

Since the total plasma pressure is expected to be limited by MHD instabilities, the increasing ash density will lead to a reduction of the fuel density and, consequently, the fusion power density.

$$W_{\rm th} = 1.5T(n_{\rm e} + 2n_{\rm D} + n_{\rm He}) = 6Tn_{\rm D}(1 + 3n_{\rm He}/4n_{\rm D}),$$

$$P_{\rm f} = 5E_\alpha\langle\sigma v\rangle_{\rm th}\left(\frac{W_{\rm th}}{6T(1 + 3n_{\rm He}/4n_{\rm D})}\right)^2 \equiv \langle\sigma v\rangle_{\rm th}\left(\frac{W_{\rm th}}{6T}\right)^2 F_{\rm d}$$

where $F_{\rm d}$ is the fusion power reduction factor due to dilution of the fuel by ash buildup (Fig. 2b).

Taking the gross electrical power density to be $\eta_{\rm th}P_{\rm f}$, the effective net electrical power density is

$$\begin{aligned} P_{\rm e,net} &= \eta_{\rm th}P_{\rm f} - P_{\rm b}/\eta_{\rm b} = \eta_{\rm th}\langle\sigma v\rangle_{\rm th}\left(\frac{W_{\rm th}}{6T}\right)^2 F_{\rm d}(1 - 1/\eta_{\rm th}\eta_{\rm b}Q) \\ &\equiv \eta_{\rm th}\langle\sigma v\rangle_{\rm th}\left(\frac{W_{\rm th}}{6T}\right)^2 F_{\rm net}, \end{aligned}$$

where F_{net} is the overall net power reduction factor due to both dilution from ash accumulation and recirculated power for the beam fueling system. Note that this power reduction will overcome the higher average fusion power density provided by peaked density profiles unless both high Q and low τ_{He}/τ_D are achieved (Fig. 2c).

At this point we can compare the relative merits of positive-ion-based neutral beams (with $\eta_b \sim 0.3$ and $E_D \sim 100$ keV) and negative-ion-based beams (with $\eta_b \sim 0.6$ and $E_D \sim 200$ keV). For fixed particle confinement times the Q is higher for the lower energy beams but the fuel dilution is the same. However, the lower electrical efficiency of positive-ion-based beams offsets their higher Q and the net electrical power densities are equal. The better beam penetration of higher voltage beams breaks the tie in favor of negative-ion-based beams for power producing devices. However, in smaller neutron sources or pilot plants the lower injected power and higher power density through vacuum vessel ports are likely to weigh heavily in favor of positive-ion-based beams.

Finally, the ratio of thermal and particle confinement times is

$$\tau_E/\tau_D = W_{th}/(\tau_D(P_b + P_\alpha)) = 6T\left(2E_\alpha/E_D - Q(1 - 0.75\tau_{He}/\tau_D)\right)/(E_\alpha(5+Q)).$$

As expected, Fig. 2d shows that high Q requires much better fuel particle confinement than thermal confinement.

In summary, good performance for a beam fueled power producing system requires $Q \geq 3/\eta_{th}\eta_b \sim 12$, $E_D \leq E_\alpha/Q \sim 200$ keV, $\tau_D \gg \tau_E$ *and* $\tau_D \gg \tau_{He}$ (but note that $\tau_{He} \gg \tau_E$ is permissible). The minimum reduction in net power due to fuel dilution and to recirculated electrical power for the beams is 30–40%. This essentially balances the increase in fusion power which arises from the peaked density profile, so the increased average power density can be sufficient — in this idealized analysis — to provide the power to run the beam fueling system.

This discussion has assumed that the beam penetration is good, i.e., all injected ions have equal chances to undergo a fusion reaction. In the next section we find that the inclusion of realistic beam deposition leads to more stringent requirements on the ratio of thermal and particle diffusivities.

2.2. 1-d Calculations of Beam Fueled Plasmas

Prior work[39] on beam fueled high Q plasmas with *a priori* peaked density profiles is compatible with the 0-d results of the previous section. It showed that the implied particle diffusivity was much lower than the thermal diffusivity, and that the central beam fueling rate was comparable to the fusion loss rate.

The goal of the 1-d simulations described here is to generate self consistent steady-state simulations of plasmas which are fueled by neutral beams and heated by the beams and fusion products. Since the 0-d model indicates that the ratio of particle and thermal confinement is a fundamental determinant of the performance we generate a sequence of plasmas with different values of the ratio of thermal diffusivity to hydrogenic particle diffusivity, χ/D_{Hy}, but with the same total stored energy. (In order to simplify the comparison we assume that the β limit is independent of

pressure peakedness.) The ash to fuel particle confinement ratio is parameterized by $D_{\mathrm{Hy}}/D_{\mathrm{He}} \propto \tau_{\mathrm{He}}/\tau_{\mathrm{D}}$ and the two diffusivity ratios are varied to find the conditions for high Q beam fueling with a peaked density profile.

Since tokamak temperature profiles are quite 'resilient' and generally well approximated by $T(r) \propto [1-(\rho/a)^2]^{\alpha_{\mathrm{T}}}$ with $1 < \alpha_{\mathrm{T}} < 2$ we assume a fixed temperature profile shape. In order to simplify the calculations we use $T_i = T_e$. We assume a central temperature of 25 keV and $\alpha_{\mathrm{T}} = 1.5$. Although low plasma density is desirable for beam penetration, good divertor performance requires a substantial edge density[40]. The edge electron density for these calculations is accordingly fixed at $3 \times 10^{19}\mathrm{m}^{-3}$. The edge helium density is 10% of n_e, and the carbon density is 2% of n_e throughout the plasma ($Z_{\mathrm{eff}} \geq 1.6$). Calculations not reported here show that reasonable variations of temperature profile shape or hydrogen and helium edge density lead to modest changes in the results.

The hydrogenic densities are calculated from a particle diffusion equation — with no pinch — involving only the beam source and the fusion sink. The helium ash source is assumed to be equal to the local fusion reaction rate — we thus assume no losses or radial diffusion of alphas as they thermalize. The fusion rate includes both beam-target and thermal-thermal reactions. Inclusion of a particle pinch would, of course, have both beneficial and undesirable effects by peaking the hydrogenic and ash density profiles, respectively.

The density profile determines the beam deposition which is, in turn, the source for the density calculation so we use an iterative algorithm with the following steps:

- the beam fueling is calculated using initial guesses for the density profile and the beam power,
- the 'effective' single-fluid thermal diffusivity is inferred from the integrated heating power minus the convected power ($1.5T$ times the particle flux from beam fueling),
- the particle diffusivity is derived from the thermal diffusivity using an input value of χ/D_{Hy}, and the density profiles for hydrogenic ions are determined by solving a 1-d radial diffusion equation,
- the density profile of helium ash is similarly determined using a helium diffusivity proportional to the hydrogenic diffusivity,
- the new density profile is used to recalculate the beam deposition and the above steps are repeated until the the hydrogenic and helium density profiles have converged,
- the total stored energy is calculated, the beam power is adjusted, and the above steps are repeated until the total stored energy converges to the desired W_{tot}.

The preceding 0-d analysis makes it clear that performance is maximized by injecting low energy beams into a plasma with small minor radius. The High Aspect

Ratio Design for ITER, HARD, is such a relatively compact tokamak[30]. This tokamak has R_o=6.3 m, a=1.6 m, κ_{95}=2, I_p=15 MA, and B_o=7.1 T, and a total stored energy of 0.37 GJ. For these calculations the core elongation of 1.65 is used for all flux surfaces. The results of the previous section suggest that a beam energy of ~50 keV might lead to a sufficiently high Q to be attractive. Unfortunately, calculations of the type described in this section show that the penetration is so poor that the peakedness of these high Q plasmas is $\sim$ 1.0, i.e. the profiles are essentially as flat as with gas puffing.

It would be desirable to develop reactor designs with even smaller minor radius so that low energy beams could fuel the core but there are two obstacles along this path:

1. conventional energy confinement scalings favor large I_p and hence higher a,
2. the blanket thickness is independent of the plasma minor radius and this causes the ratio of the plasma volume to the blanket volume (and the fusion power per unit cost) to fall with declining a.

A full scale systems code is needed to properly optimize a beam feuled reactor, but this is beyond the scope of the present work.

For the calculations reported here we use 200(300) keV D(T) beam fueling in one of the smallest available reactors, HARD. This beam voltage is adequate to produce a density peaking of 2. The D:T beam power and voltage ratios are fixed at 2:3 in order to provide equal particle source rates; the quasi-perpendicular injection radius is R_{tang}=1 m.

Results from these 1-d simulations with E_D=200 keV, $\langle T_i \rangle_n = \langle T_e \rangle_n$=15 keV, for D_{Hy}/D_{He} = 0.2 are in general agreement with the 0-d model. As expected Q rises with increasing χ/D_{Hy}, but τ_D/τ_E increases more slowly than χ/D_{Hy} (Fig. 3a). This sublinear behaviour occurs because as Q rises the fusion loss rate of fuel ions becomes appreciable and it flattens the effective particle source profile; this tendency is 'amplified' as the broader density profile causes the beam deposition profile to be broader. The density peakedness varies from 2.7 to 1.9 for $10 < \chi/D_{Hy} < 100$. The increasingly broader fuel source profile causes τ_D to rise more slowly than $1/D$; this also causes τ_{He}/τ_D to rise from $\sim 1 \rightarrow 2D_{Hy}/D_{He}$ as χ/D_{Hy} rises from 10 to 100 (Fig. 3a). For the 1-d model a given Q requires somewhat lower τ_D/τ_E than the 0-d model (Fig. 3b), but the values of χ/D_{Hy} which are required for high Q are larger than the τ_D/τ_Erequired by the 0-d model. Also as anticipated, the helium ash fraction rises with increasing χ/D_{Hy}; near the 'average' radius of $r = a/2$ the results are in reasonable agreement with the 0-d model (Fig. 3c). Avoiding serious fusion power reductions for high Q plasmas again requires very different particle diffusivities for helium and hydrogenic species: $D_{He} \gg D_{Hy}$.

By varying the helium and hydrogenic diffusivities separately we find that $D_{He} = \chi/10$ is sufficient to permit high Q operation without serious fusion power reduction; i.e., the diffusivity of the helium can be low — relative to χ — without leading to catastrophic fuel dilution. Unfortunately, while $D_{He} \sim \chi$ has been reported from a number of tokamaks[41,42], the available data are not sufficient to demonstrate that

large helium diffusivities can occur simultaneously with low hydrogenic diffusivities. Recently, the measurements of $\chi/D_{\mathrm{He}} \sim 1-3$ obtained for L-modes and supershots in TFTR have been used to infer a steady-state helium profile for ITER which would not adversely affect the plasma reactivity[43,44]. If the desired level of helium transport does not occur naturally it may be possible to move the alphas toward the plasma edge with external systems[45–47].

Profiles from a simulation with $\chi/D_{\mathrm{Hy}} = 100$ and $D_{\mathrm{Hy}}/D_{\mathrm{He}} = 0.2$ illustrate the various profiles. The hydrogenic beam fueling source (Fig. 4a) in our beam fueled simulations is peaked well off-axis as a result of the poor penetration of 200 keV beams in large dense plasmas. Note that in spite of the broad source profile and large fusion loss rate near $r \sim 0$ the density profile is peaked (Fig. 4b). (Even if the net source were zero in the core the density profile would be flat in the source-free region.) It is remarkable that this occurs for a diffusivity profile which is nearly flat in the core of the plasma (Fig. 4c); with the very hollow diffusivity profiles found in some peaked profile discharges with very good core confinement[23] the density profile would be much more peaked than shown here. The helium source, and thus the helium density, are much more centrally peaked.

Values of $1 < \chi/D < 10$ have been observed[6,48,49] (it should be noted, however, that their definitions differ in detail from those used here). Supershots, in particular, have very peaked profiles but their convectively dominated cores[50] with $\chi/D \leq 1$ do not provide the conditions for high Q operation. Very large ratios, $\chi/D \sim 100$, have not been reported but the implied particle diffusivities are of the same order as the neoclassical diffusivities in large tokamaks and may be achievable if 'anomalous' transport processes can be suppressed.

While the net electric power of a beam fueled system with a peaked density profile may not be significantly higher than that of plasma with a flat density profile there are other reasons for considering beam injection. Driven systems can tolerate higher impurity levels[37] and also have an inherent means of burn control, pressure profile control and, hence, bootstrap current control. This in turn, could lead to improved MHD stability, higher operating pressure, and higher fusion power. The added cost of the beam system should therefore be compared to that of alternative systems for achieving these ends in order to assess the relative advantages of the two approaches.

3. Core fueling by pellet injection

In contrast to neutral beam fueling, pellet injection requires negligible power and differs in its dependence on plasma density and temperature. The largest handicap of neutral beam fueling, recirculated power, is no problem at all for pellet fueling because the average energy expended per particle is quite small. The largest uncertainty is the feasibility of making pellet injectors with sufficiently high speed to deposit much of the pellet mass deep in the plasma. It is not necessary, however, to deposit most of the particles very near the plasma center because particle diffusion can be counted on to move particles to the center while they are removed from the outer part of the plasma.

This scenario has been observed in TFTR discharges with partial penetration of multiple pellets[51,52]. After each pellet was deposited particle diffusion filled in the center of the density profile while the density in the outer regions declined and the profile became moderately peaked (Fig. 5). (The neutral beam fueling rate was less than 5% of $\dot{n}_e$ while the core density was rising in the region $r < 0.2$ m.) The density peakedness repeatedly returned to $n_{eo}/\langle n_e \rangle \simeq 2$ as the density in the outer regions diffused away. Since the density profile is periodically flattened locally in the core this fueling scenario may not be sufficient to suppress sawteeth at all times via ω_* stabilization[53].

The neutral gas shielding model[54] for pellet ablation used below accounts for the measured pellet penetration depth in JET experiments[55], but the radial profile of the change in density following the pellet event is somewhat shallower than predicted[56]. Furthermore, in auxiliary heated discharges up to half the particles in the pellet appear to leave the plasma very quickly. In practice, therefore, one would use larger pellets than in the present simulations. This would compensate for both the missing particles and the broader than expected deposition profile, i.e., the calculations reported here should be viewed as representing the actual deposition from pellets containing twice as many particles as those used in the calculation. This need to use larger pellets should cause no difficulty for the overall plant power balance since the energy cost per particle is negligible, but it might affect the tritium inventory and the pumping requirement.

The neutral gas shielding model for pellet ablation provides to an estimate of the fractional penetration[55] in terms of the pellet speed and radius, the central electron density and temperature, and the horizontal minor radius of the plasma:

$$\lambda/a \propto \left(\frac{v_{\rm pel} r_{\rm pel}^{5/3}}{a n_{eo}^{1/3} T_{eo}^{5/3}} \right)^{\gamma},$$

for density and temperature profiles proportional to $[1 - \rho/a]^{\alpha}$ and where $\gamma \equiv 3/(3 + \alpha_n + 5\alpha_T)$. Pellet penetration is enhanced strongly at low electron temperature, but depends only weakly on plasma density. The key to improving pellet penetration is therefore to use the lowest electron temperature which is compatible with other constraints.

The other major factors determining penetration are the pellet size and speed. The size is constrained by the allowable change in the number of ions, which in turn is determined by the allowable change in the fusion power or the density limit. Large excursions in fusion power lead to thermal oscillations in the tokamak and blanket which could cause structural 'fatigue'. For fixed major radius, penetration is almost independent of plasma minor radius because the permissible pellet size increases with plasma volume. At constant plasma minor radius the pellet size can be increased by raising the major radius, elongation, or the toroidal magnetic field strength (the average density rises with B_{tor}). As with neutral beam injection, a large Shafranov shift is helpful since it minimizes the distance between the core and the outboard edge of the plasma.

Penetration to the center of conventional reactor designs requires pellet speeds of

10–15 km/sec[54] but present day experiments show that deep penetration to the core, $r \sim a/3$, is sufficient to produce a significantly peaked density profile. By using deep penetration and by reducing the temperature of the target plasma it becomes possible to produce a peaked density profile in a reactor with pellet speeds of 5–10 km/sec. This can be done without significantly reducing the fusion power by operating near the optimal temperature (Fig. 1).

It is not uncommon for pellets to increase the number of particles in present day plasmas by factors of 2–3, but such a large change in density would necessarily cause a large change in the fusion power which would lead to undesirable thermal transients in the surrounding tokamak structural components and in the neutron absorbing blanket. We have therefore examined smaller changes in density with $\Delta N/N$ <1. For pellets with a modest fractional density increase, $\Delta N/N$ =~0.2–0.5, the target plasma temperature should be on the low temperature side of the reactivity curve (see Fig. 1); even after the pellet decreases the average temperature the fusion power can be above the level produced by broad density profiles. For large pellets with a fractional density increase $\Delta N/N$ =~0.5–1 the target plasma temperature should be near or above the optimal temperature; again, after the temperature reduction the fusion power remains high. Even with this strategy higher pellet speeds are preferable since the fusion power can be maintained near the maximum with smaller pellets and, hence, smaller changes in density and fusion power.

In order to quantitatively evaluate these strategies we have used the PELLET code[55] to calculate the change in fusion power in HARD[30] for pellets which increase the average electron density by 20 and 60%. Its higher toroidal magnetic field strength and larger fractional Shafranov shift make it more attractive for core pellet fueling than the ITER/CDA. In these calculations the pre-pellet target density is proportional to $[1-(\rho/a)^2]$ and the target temperature is proportional to $[1-(\rho/a)^2]^{1.5}$. We assume T_i=T_e; the pellets while the hydrogenic plasma ions are composed of a 50:50 D:T mix. The thermal stored energy and impurity dilution are maintained at the levels in the standard HARD ignition scenario as the target temperature and density are varied (the pellet size is adjusted to follow the corresponding change in density). When pellets do not fully penetrate the immediate post-pellet density profile is typically 'hollow' (Fig. 6) and the core temperature remains high. In order to estimate the full change in fusion power which would occur after the hollow density profile has filled in, the post-pellet density and temperature profiles have been flattened (conserving particles and energy) inside the radius where the local density equals the interior average density:

$$n_e(r) = 2/r^2 \int_0^r n_e(r')r' \, dr'.$$

We find that pellets which reach $r \sim 0.35a$ are sufficient to maintain the peakedness of the assumed target density profile when the target density and temperature are chosen carefully for each pellet size and speed; the results for these cases are shown in Fig. 7. There is remarkably little difference in the average fusion power for small or large density changes; even for speeds of 5–10 km/sec the fusion power changes only 10–15% and remains higher than that of the nominal HARD ignition scenario.

This brings the required speed much closer to the range of existing pellet injectors. At 15 km/sec it would be possible to maintain peaked density profiles with modest changes in density and essentially no change in fusion power, but pellet speeds this high do not appear to be necessary in order to maintain peaked density profiles.

While the preceding calculations are useful in scoping out the pellet fueling scenario we need a more complete simulation of the density and temperature evolution after pellet injection. In particular, we need more physical estimates of the evolution of 1) the density profile and 2) the fusion power as the density profile relaxes and the temperature responds to the changing alpha heating power (the thermalization time scale and the 'birth' rate vary). This has been provided by a simulation of refueling with large, fast pellets (pellet radius = 0.725 cm, pellet velocity = 7 km/sec) in the ITER EDA (with R=8.11 m, a=3.00 m, I_p=24MA, B_{tor}=5.7T) using the WHIST 1.5 D transport code[14]. Pellets with a 50-50 D-T mix were injected whenever the total number of ions in the plasma fell below a fixed target value by more than half of the number of atoms in a pellet. This choice of pellet size and plasma target density produced $\Delta N/N = 0.22$. The pellet deposition was computed by the neutral gas shielding model[55] used above. The code evolves profiles of electron temperature, ion temperature, and the density of three species of thermal ions: deuterium, tritium and helium.

The assumed transport model has two parts: anomalous transport according to the ITER 89-P model[57] and the full neoclassical treatment of Hinton and Hazeltine[58]. The anomalous diffusivities are assumed to have a radial profile proportional to $(1 + 4\rho^2/a^2)$ and the thermal diffusivities are normalized (as a function of time) to produce global energy confinement equal to the ITER 89-P L-mode scaling. The particle diffusion coefficient, D, was the same for all ion species, and the relationship between the anomalous thermal and particle diffusivities was taken to be $\chi_e = \chi_i = 2D$. As noted in the previous section, considerably larger ratios of χ/D are sometimes observed[6,48,49], but we expect simulations based on a higher ratio to differ only by having a longer timescale for density evolution and a correspondingly longer interval between pellet injection. In particular, the amplitude of the variation in fusion power and the depth of pellet penetration should not be affected.

At the wall, a gradient boundary condition with a 5 cm characteristic length was applied for both T_e and T_i. Since the wall is separated from the bulk plasma by a 5 cm scrape-off layer, the conditions there have a very weak influence on core plasma behavior. Transport in the scrape-off layer is treated analogously to the core plasma, but with the addition of a loss term representing parallel flow to a divertor collector.

In addition to the explicit simulation of helium ash buildup it was assumed that beryllium density was 4% of the local electron density; as a result the total Z_{eff} was $\sim$ 1.5 at all radii. All of the flow of hydrogenic ions to the wall is recycled as neutral gas; the radial source profile of neutral ionization is computed using a 1-D slab model. The neutral recycling within the divertor region is implicitly modeled in the simulation by adjusting the ion parallel flow loss rate to match the specified pump throughput (there is no neutral flux from the divertor back to the plasma). The pump throughput used for these simulations was 0.8 bar-liter/sec (4.24×10^{22} atoms/sec) which is below the ITER design value of 1 bar-liter/sec. The separatrix density produced by these

transport assumptions, $8 \times 10^{19} m^{-3}$, is close to the Borrass density limit for ITER[59].

The instantaneous fusion power in the time dependent pellet fueled simulation shows (Fig. 8) larger oscillations caused by sawteeth and smaller changes caused by pellets ($\pm 10\%$ from the average value). A somewhat smaller change is shown in Fig. 7 for this pellet speed; the difference is probably due to the lower average temperature, $\langle T_e \rangle_n \simeq \langle T_i \rangle_n = 4.2$ keV, in the time dependent simulation which has lead to deeper pellet deposition and larger changes in the core density. By operating with a lower average density and a higher temperature closer to the optimal temperature, the change in fusion power could probably be made smaller. The fusion power recovers rapidly after each pellet because the higher density and lower electron temperature cause more rapid heating of the thermal plasma by the preexisting suprathermal alpha population. The density diffuses in both directions away from the off axis peak in the pellet deposition; the central density rises by $\sim 10\%$ while most of the particles diffuse out of the plasma in a manner which resembles the density evolution shown for TFTR in Fig. 5.

We conclude that core fueling with cryogenic pellet injection could effectively produce peaked density profiles — without the considerable cost of recirculated power needed by neutral beam fueling. While developing injectors with speeds > 5 km/s is a demanding challenge it is desirable because they would raise the average density peaking that could be achieved and enable the use of smaller pellets to reduce the variation in fusion power. A recent review[60] has shown that the speeds achieved with experimental accelerators in the laboratory and with working injectors on tokamaks have steadily increased as more advanced pellet injection systems have been developed. Speeds above 3 km/sec are now achieved routinely with fueling systems based on the two-stage light-gas gun accelerator. Such a device has set the speed record for hydrogenic pellets - 4.3 km/sec - and demonstrated reliable separation of pellet and protective sabot[61]. Projectile speeds in the desired range have already been achieved in non-fusion applications with two-stage light-gas guns and electromagnetic rail gun launchers and it is not unreasonable to hope that this level of performance could be realized in tokamak fueling systems as well.

4. Conclusion

The potential for producing peaked density profiles in large tokamaks has been assessed with 0-d and 1-d plasma simulations. The use of neutral beam and pellet injectors for this purpose has often been dismissed by noting the severe requirements for producing centrally peaked *source* profiles, i.e., very high beam energies, $\sim$1 MeV, and pellet speeds, $\sim$10–15 km/sec. Since broad *source* profiles are adequate to produce peaked *density* profiles we find that more feasible injectors, 100–200 keV beams and $\sim$7 km/sec pellets, are sufficient to produce peaking factors $\sim$2.

We find that it is possible, in principle, to produce a peaked density profile in a high Q large tokamak using neutral beam fueling *if the particle diffusivity is $\sim$50–100 times lower than the thermal diffusivity.* Such a large difference between particle and thermal confinement is not seen in current tokamaks — the required particle

diffusivity is of the same order of magnitude as neoclassical diffusivity — so neutral beam fueling appears to be practically restricted to lower Q devices such as neutron sources and pilot plants[34–36].

Pellet fueling, on the other hand, involves no significant power consumption and provides an attractive way of creating peaked density profiles. The variations in the fusion power can be minimized if injection speeds are raised by continuing to pursue promising injector technologies[60].

These results are encouraging and should prompt further studies of density peaking which would fit naturally into the search for 'advanced tokamak' plasma regimes with profile control for plasma optimization. The incorporation of the features of peaked density profiles and the characteristics of selected fueling methods in tradeoff studies should lead to optimized designs which can more fully realize the improvements sought in advanced tokamaks.

5. Acknowledgements

It is a pleasure to thank L. R. Baylor, R. V. Budny, W. S. Cooper, D. Ehst, R. J. Hawryluk, D. Q. Hwang, J. Manickam, and M. C. Zarnstorff for their helpful discussions. This work was supported by U.S. DoE Contract No. DE-AC02-76-CHO-3073.

References

[1] KESNER, J. and CONN, R. W., Nucl. Fusion **16** (1976) 397.

[2] PERKINS, L. J. et al., ITER parametric analysis and operational performance, Technical Report ITER Documentation Series No. 22, IAEA, 1991.

[3] MIKKELSEN, D. R. et al., Centrally fuelled tokamaks and implications for ITER, in *Plasma Physics and Controlled Nuclear Fusion Research (Proc. 14th Int. Conf., Wurzburg, 1992)*, volume 3, pp. 463–474, Vienna, 1992, IAEA.

[4] BUDNY, R. V. et al., Nucl. Fusion **32** (1992) 429.

[5] BICKERTON, R. J. et al., Latest JET results and future prospects, in *Plasma Physics and Controlled Nuclear Fusion Research (Proc. 12th Int. Conf., Nice, 1988)*, volume 1, p. 41, Vienna, 1989, IAEA.

[6] EFTHIMION, P. C. et al., Phys. Fluids B **3** (1991) 2315.

[7] POMPHREY, N., Bootstrap dependence on plasma profile parameters, Technical Report PPPL-2854, PPPL, 1992.

[8] LEVINTON, F. M. et al., submitted to Phys. Rev. Letters.

[9] HIVELY, L. M. and MIKKELSEN, D. R., Fusion Tech. **10** (1986) 58.

[10] STOTLER, D. P., POST, D., and BATEMAN, G., Fusion Tech. **14** (1988) 1304.

[11] COPPI, B., NASSI, M., and SUGIYAMA, L., Physica Scripta **45** (1992) 112.

[12] KESSEL, C., MANICKAM, J., REWOLDT, G., and TANG, W. M., Phys. Rev. Lett. **72** (1994) 1212.

[13] MANICKAM, J., (1994), private communication.

[14] HOULBERG, W. A. et al., Nucl. Fusion **34** (1994) in press.

[15] MEADE, D. M. et al., Recent TFTR results, in *Plasma Physics and Controlled Nuclear Fusion Research (Proc. 13th Int. Conf., Washington, 1990)*, volume 1, pp. 9–26, Vienna, 1991, IAEA.

[16] ISHIDA, S. et al., High poloidal beta experiments with a hot ion enhanced confinement regime in the JT-60 tokamak, in *Plasma Physics and Controlled Nuclear Fusion Research (Proc. 13th Int. Conf., Washington, 1990)*, volume 1, pp. 195–207, Vienna, 1991, IAEA.

[17] NAVRATIL, G. A. et al., Study of high poloidal beta plasmas in TFTR and DIII-D, in *Plasma Physics and Controlled Nuclear Fusion Research (Proc. 13th Int. Conf., Washington, 1990)*, volume 1, pp. 209–218, Vienna, 1991, IAEA.

[18] SABBAGH, S. A. et al., Phys. Fluids B **3** (1991) 2277.

[19] POLITZER, P. A., Phys. Plasmas **1** (1993) in press.

[20] SCHMIDT, G. L. et al., Pellet injection results during TFTR ohmic and neutral beam heating experiments, in *Plasma Physics and Controlled Nuclear Fusion Research (Proc. 11th Int. Conf., Kyoto, 1986)*, volume 1, pp. 171–178, Vienna, 1987, IAEA.

[21] JET Team, Heating of peaked density profiles produced by pellet injection in JET, in *Plasma Physics and Controlled Nuclear Fusion Research (Proc. 12th Int. Conf., Nice, 1988)*, volume 1, pp. 215–228, Vienna, 1989, IAEA.

[22] TUBBING, B. J. D. et al., Nucl. Fusion **31** (1991) 839.

[23] BAYLOR, L. R. et al., Nucl. Fusion **31** (1991) 1249.

[24] KAMADA, Y. et al., Nucl. Fusion **31** (1991) 23.

[25] ZARNSTORFF, M. C. et al., Phys. Rev. Lett. **60** (1988) 1306.

[26] KIKUCHI, M. et al., Nucl. Fusion **30** (1990) 343.

[27] ONO, M. et al., OH density peaking with IBW, in *Proceedings of the 9th Topical Conference on Radio-frequency Power in Plasmas, Charleston, 1991*, volume AIP Conference Proceedings 244, p. 223, American Institute of Physics, New York, 1992.

[28] PERKINS, L. J., HO, S. K., and HAMMER, J. H., Nucl. Fusion **28** (1988) 1365.

[29] HO, S. K. and THE ARIES TEAM, Controlled central fueling for ARIES-III by compact toroid injection, in *Proceedings of the 14th IEEE/NPSS Symposium on Fusion Engineering, San Diego, 1991*, volume 1, p. 205, IEEE, 1992.

[30] WESLEY, J. C. and THE U. S. ITER HOME TEAM, Fusion Tech. **21** (1992) 1380.

[31] EHST, D. et al., Tokamak power systems studies - FY 1986: A second stability power reactor, Technical Report ANL/FPP/86-1, ANL, 1987, p. 7-26, ff.

[32] EHST, D. et al., Tokamak power systems studies: A second stability power reactor, in *Proc. 12th Symposium on Fusion Engineering (Monterey, 1987)*, volume 1, pp. 489–492, Piscataway, 1987, IEEE.

[33] COOPER, W. S., Phys. Fluids B **4** (1992) 2300.

[34] DEAN, S. O. et al., J. Fusion Energy **11** (1992) 85.

[35] GALAMBOS, J. et al., Fusion Tech. **21** (1992) 1759.

[36] DEAN, E. J. et al., Pilot plant: A shortened path to fusion power, in *Plasma Physics and Controlled Nuclear Fusion Research (Proc. 14th Int. Conf., Wurzburg, 1992)*, volume 3, pp. 355–360, Vienna, 1992, IAEA.

[37] CONN, R. W. and KESNER, J., Nucl. Fusion **15** (1975) 775.

[38] REITER, D., WOLF, G. H., and KEVER, H., Nucl. Fusion **30** (1990) 2141.

[39] BUDNY, R. V. et al., Simulations of beam-fueled supershot-like plasmas near ignition, in *Conference on Controlled Fusion and Plasma Physics (Proc. 19th Int. Conf., Innsbruck, 1992)*, volume 16C, part 1, pp. 43–46, Brussels, 1992, EPS.

[40] COHEN, S. A. et al., Power and particle control for ITER, in *Plasma Physics and Controlled Nuclear Fusion Research (Proc. 13th Int. Conf., Washington, 1990)*, volume 1, pp. 321–330, Vienna, 1991, IAEA.

[41] SYNAKOWSKI, E. J. et al., Phys. Rev. Lett. **65** (1990) 2255.

[42] HOGAN, J. T. et al., Nucl. Fusion **31** (1991) 2181.

[43] SYNAKOWSKI, E. J. et al., Particle and energy transport studies on TFTR and implications for helium ash in fusion devices, in *Plasma Physics and Controlled Nuclear Fusion Research (Proc. 14th Int. Conf., Wurzburg, 1992)*, volume 1, pp. 541–550, Vienna, 1992, IAEA.

[44] SYNAKOWSKI, E. J. et al., Phys. Fluids B **5** (1993) 2215.

[45] CHANG, C. S., LEE, J.-Y., and WEITZNER, H., Phys. Fluids B **3** (1991) 3429.

[46] MYNICK, H. E., Phys. Fluids B **5** (1993) 2460.

[47] MYNICK, H. E. and POMPHREY, N., Swept alpha removal, Technical Report PPPL-2970, PPPL, 1994, submitted to Nuclear Fusion.

[48] CHEETHAM, A. D. et al., Measurements of correlations between thermal and particle transport in JET, in *Plasma Physics and Controlled Nuclear Fusion Research (Proc. 13th Int. Conf., Washington, 1990)*, volume 1, p. 483, Vienna, 1991, IAEA.

[49] EFTHIMION, P. C. et al., Phys. Rev. Lett. **63** (1991) 421.

[50] ZARNSTORFF, M., GOLDSTON, R., BELL, M., et al., Transport analysis of TFTR supershots, in *Proceedings of the 16th European Conference on Controlled Fusion and Plasma Heating, Venice, 1989*, volume 1, pp. 35–38, European Physical Society, Petit-Lancy, Switzerland, 1989.

[51] SCHMIDT, G. L. et al., Fuelling of JET limiter and X-point plasmas by pellet injection, in *Conference on Controlled Fusion and Plasma Physics (Proc. 19th Int. Conf., Innsbruck, 1992)*, volume 16C, part 1, pp. 255–258, Brussels, 1992, EPS.

[52] BELL, M. G. et al., Nucl. Fusion **32** (1992) 1585.

[53] ZAKHAROV, L., ROGERS, B., and MIGLIUOLO, S., Phys. Fluids B **5** (1993) 2498.

[54] PARKS, P. B. and TURNBULL, R. J., Phys. Fluids **21** (1978) 1735.

[55] HOULBERG, W. A. et al., Nucl. Fusion **32** (1992) 1951.

[56] BAYLOR, L. R. et al., Nucl. Fusion **32** (1992) 2177.

[57] UCKAN, N. A. et al., Energy and particle confinement in ITER, in *Plasma Physics and Controlled Nuclear Fusion Research (Proc. 13th Int. Conf., Washington, 1990)*, volume 3, p. 307, Vienna, 1991, IAEA.

[58] HINTON, F. L. and HAZELTINE, R. D., Rev. Mod. Phys. **48** (1976) 239.

[59] COMMITTEE, I. T. A., Detail of the iter outline design report, summary and overall physics issues, Technical Report TAC-4-03, PPPL, 1993.

[60] COMBS, S. K., Rev. Sci. Instrum. **64** (1993) 1679.

[61] KUPSCHUS, P., SONNENBURG, K., W.BAILEY, et al., The JET high-speed pellet launcher prototype — development, implementation and operational experience, in *Fusion Technology 1990 (Proceedings of the 16th Symposium, London, 1990*, volume 1, p. 268, North Hollod, Amsterdam, 1991.

6. Figure Captions

1) The fusion power density vs. average temperature for broad and peaked density profiles (temperature proportional to $(1-(r/a)^2)^{\alpha_T}$ with $\alpha_T = 1.5$ for the solid curves, and 1.0 for the dashed curves, B_o=5 T, β_{tor}=6%).

2) Results of the 0-d model with E_D=200 keV, $\eta_b = 0.6$, $\eta_{th} = 0.4$, $T = 15$ keV, for τ_{He}/τ_D=1.0, 0.5, 0.2, and 0.1: a) the ratio of helium and deuterium densities, b) the fusion power reduction factor due to dilution, c) the net electrical power reduction factor, d) the ratio of fuel particle and energy confinement times.

3) Results from the 1-d simulations of beam fueling in HARD with E_D=200 keV, $\langle T_i\rangle_n$=$\langle T_e\rangle_n$=15 keV, for $D_{Hy}/D_{He} = 0.2$ compared with some of the 0-d results described in Figure 2: a) the ratio of fuel particle and energy confinement times and the ratio of ash and fuel particle confinement times as functions of the ratio of thermal and fuel particle diffusivities, b) the ratio of fuel particle and energy confinement times as a function of Q for the 1-d and 0-d models, c) the ratio of helium and deuterium densities as a function of Q for the 1-d model (at $r = 0$ and $r = a/2$) and the 0-d model.

4) Profiles from a 1-d simulation with E_D=200 keV, $\langle T_i\rangle_n$=$\langle T_e\rangle_n$=15 keV, $\chi/D_{Hy} = 100$, and $D_{Hy}/D_{He} = 0.2$: (a) the deuterium and helium particle source rates, (b) their density, and (c) the effective thermal diffusivity.

5) The electron density profiles for a TFTR discharge immediately prior to and following pellet deposition which peaked the density off-axis.

6) The electron density profiles for simulations of pellet deposition in HARD.

7) The fusion power vs $\langle T_i\rangle_n$ for HARD using pre-pellet, post-pellet, and 'filled in' profiles (the pre-pellet points lie on the solid line) for three choices of pellet speed and the pellet size chosen to produce (a) $\Delta N/N = 0.2$, and (b) $\Delta N/N = 0.6$.

8) (a) The fusion power vs time for a WHIST simulation of the ITER EDA tokamak refueled by pellets injected at 7 km/sec producing $\Delta N/N = 0.22$, (b) the density evolution after pellet injection relaxes to the pre-pellet profile.

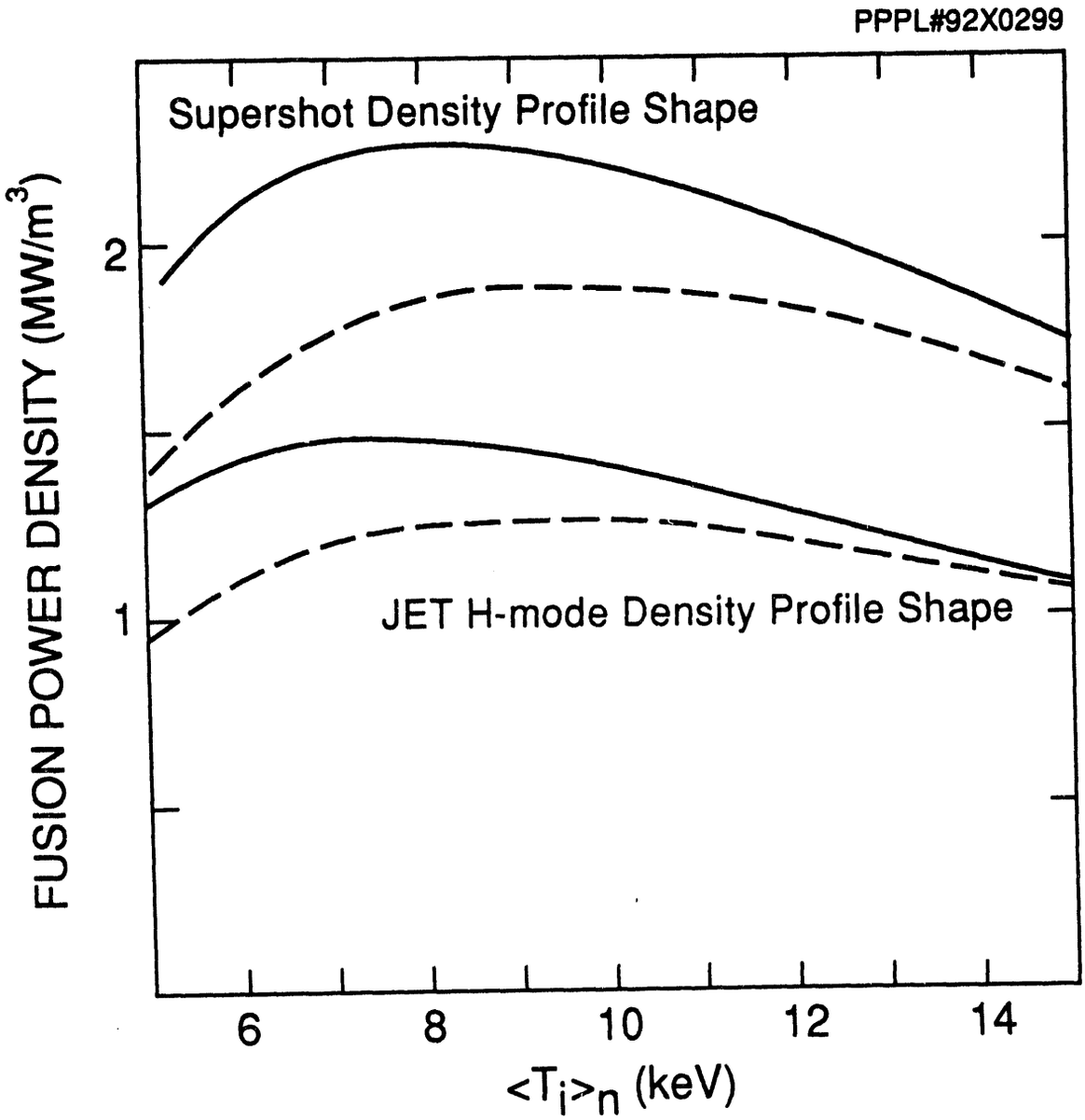
PPPL#92X0299
Supershot Density Profile Shape
JET H-mode Density Profile Shape
FUSION POWER DENSITY (MW/m^3)
2
1
6
8
10
12
14
$<T_i>_n$ (keV)

Figure 1

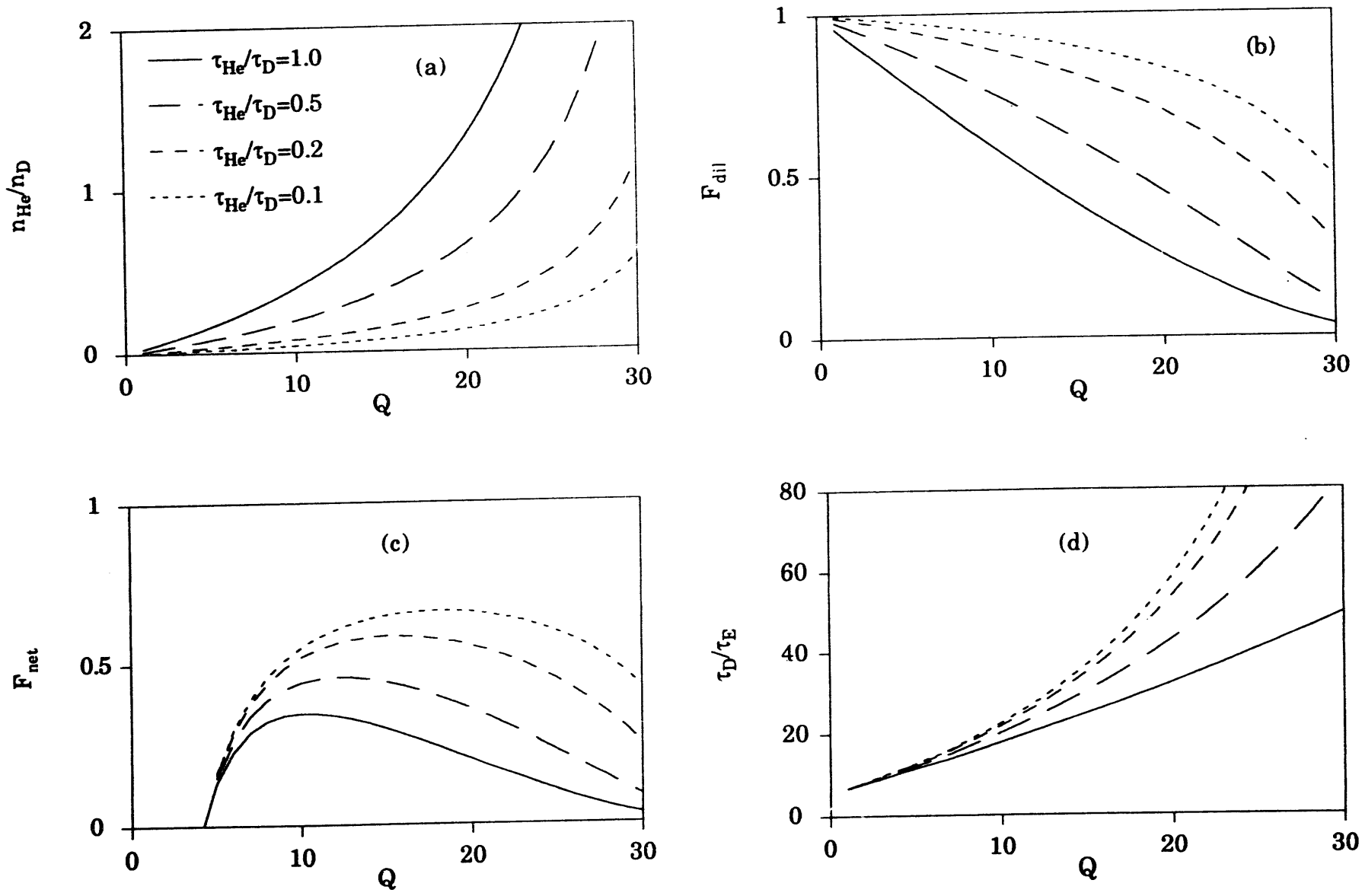
(a)
τ_{He}/τ_D=1.0
τ_{He}/τ_D=0.5
τ_{He}/τ_D=0.2
τ_{He}/τ_D=0.1
n_{He}/n_D
Q
(b)
F_{dil}
Q
(c)
F_{net}
Q
(d)
τ_D/τ_E
Q

Figure 2

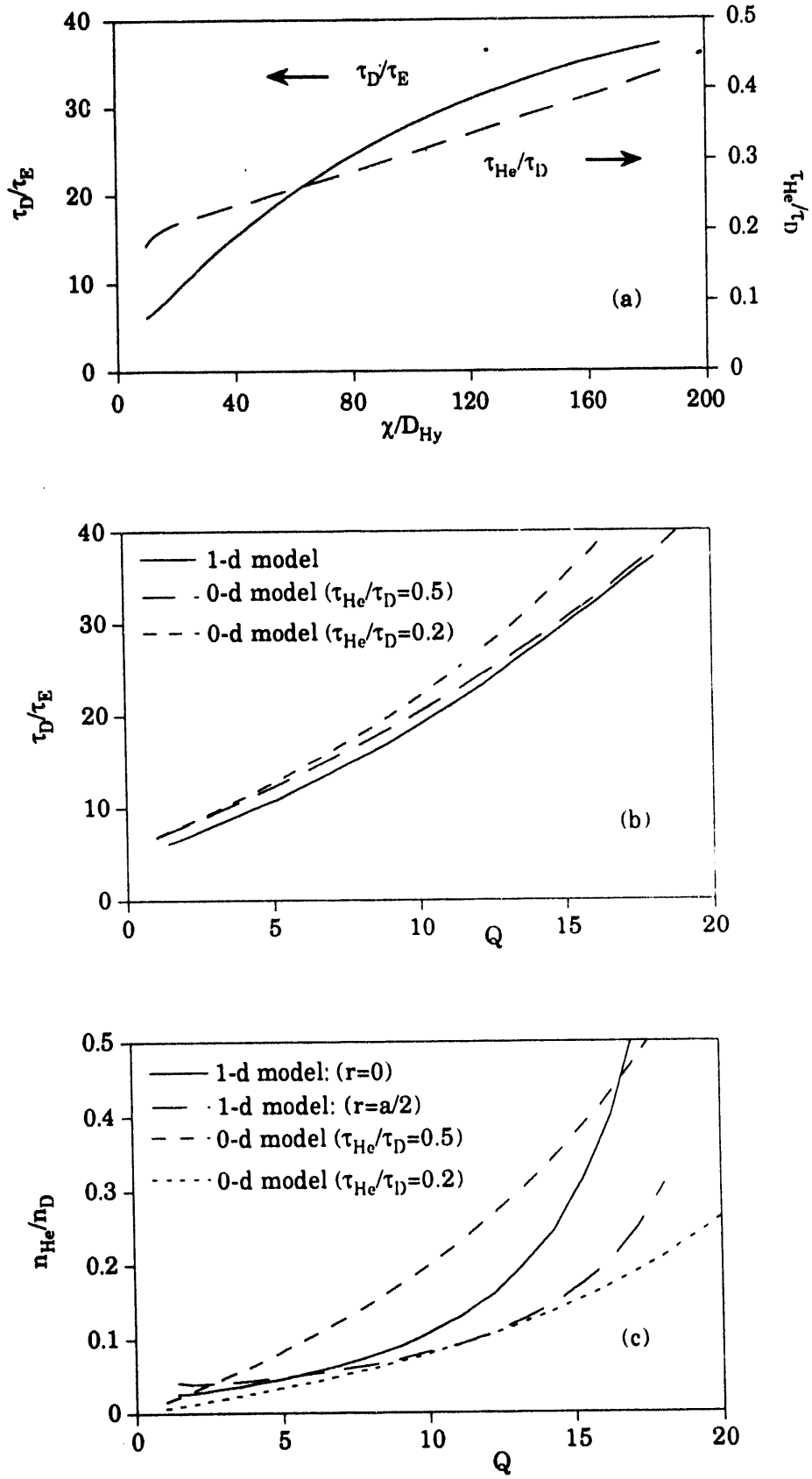
τ_D/τ_E
τ_{He}/τ_D
(a)
χ/D_{Hy}
1-d model
0-d model (τ_{He}/τ_D=0.5)
0-d model (τ_{He}/τ_D=0.2)
(b)
Q
1-d model: (r=0)
1-d model: (r=a/2)
0-d model (τ_{He}/τ_D=0.5)
0-d model (τ_{He}/τ_D=0.2)
n_{He}/n_D
(c)
Q

Figure 3

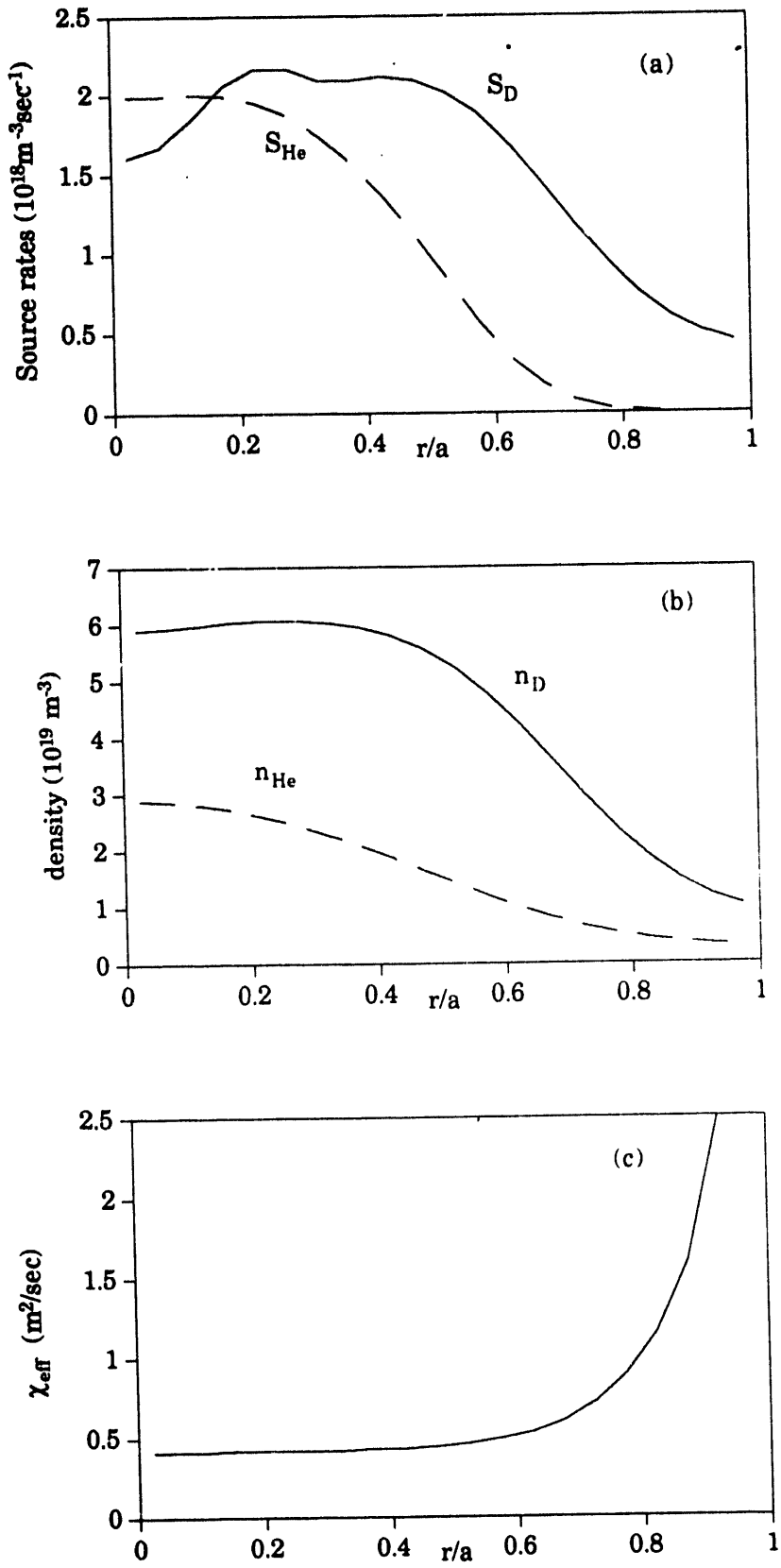
(a)
S_D
S_{He}
Source rates ($10^{18}m^{-3}sec^{-1}$)
r/a
(b)
n_D
n_{He}
density (10^{19} m^{-3})
r/a
(c)
χ_{eff} (m^2/sec)
r/a

Figure 4

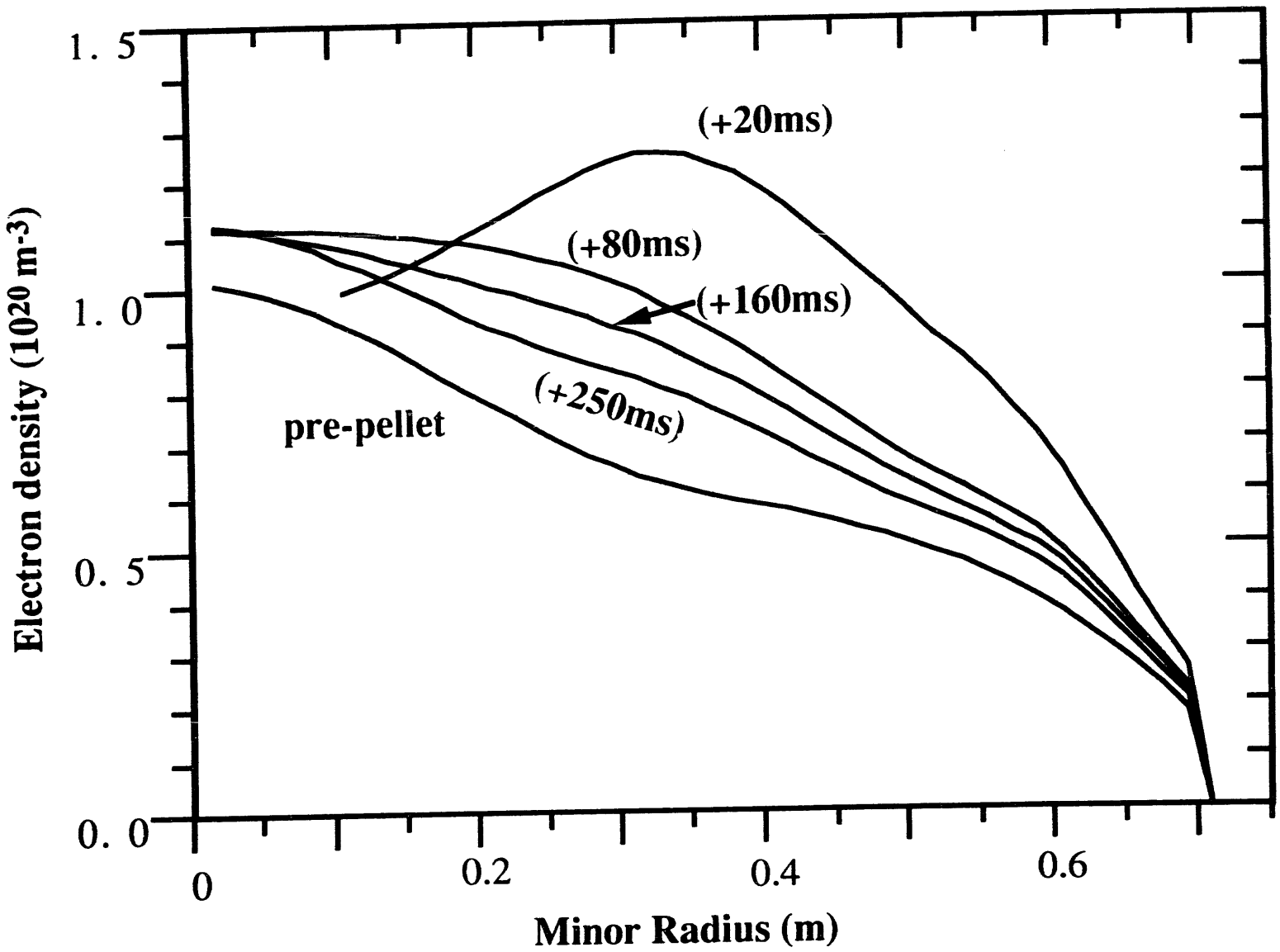
1. 5
1. 0
0. 5
0. 0
Electron density (10^{20} m^{-3})
0
0.2
0.4
0.6
Minor Radius (m)
(+20ms)
(+80ms)
(+160ms)
(+250ms)
pre-pellet

Figure 5

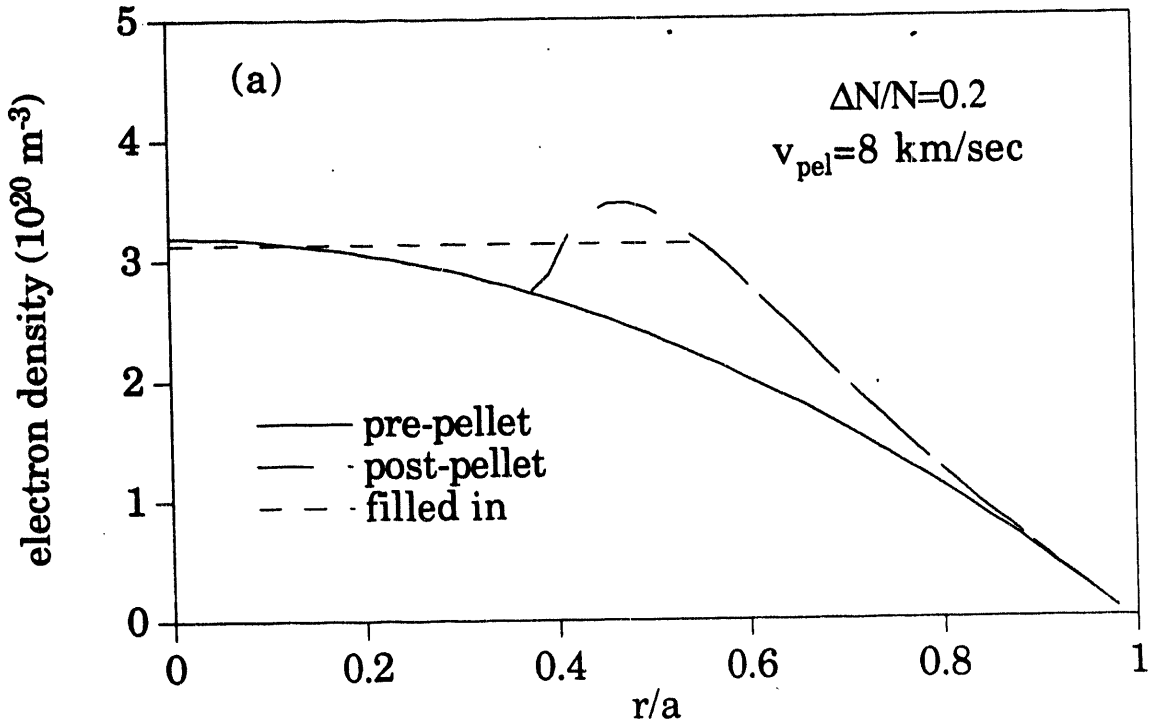
(a)
ΔN/N=0.2
v_pel=8 km/sec
pre-pellet
post-pellet
filled in
electron density (10^20 m^-3)
r/a
0
1
2
3
4
5
0.2
0.4
0.6
0.8

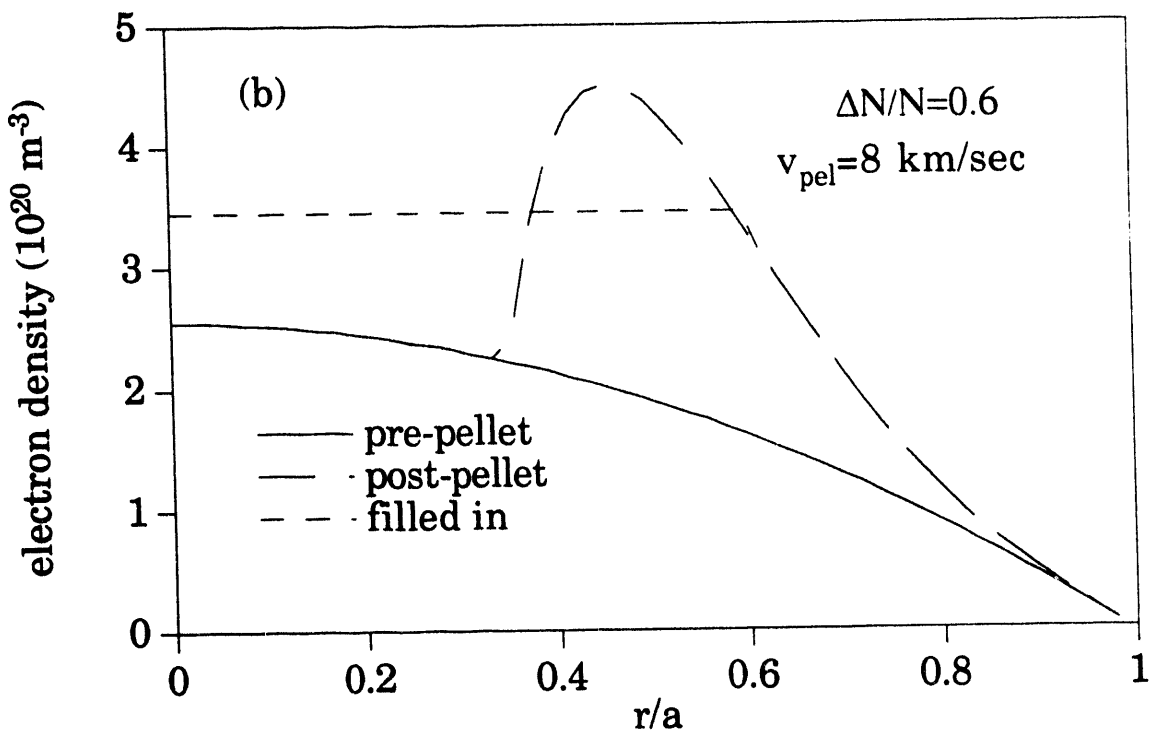
(b)
ΔN/N=0.6
v_pel=8 km/sec
pre-pellet
post-pellet
filled in
electron density (10^20 m^-3)
r/a
0
1
2
3
4
5
0.2
0.4
0.6
0.8

Figure 6

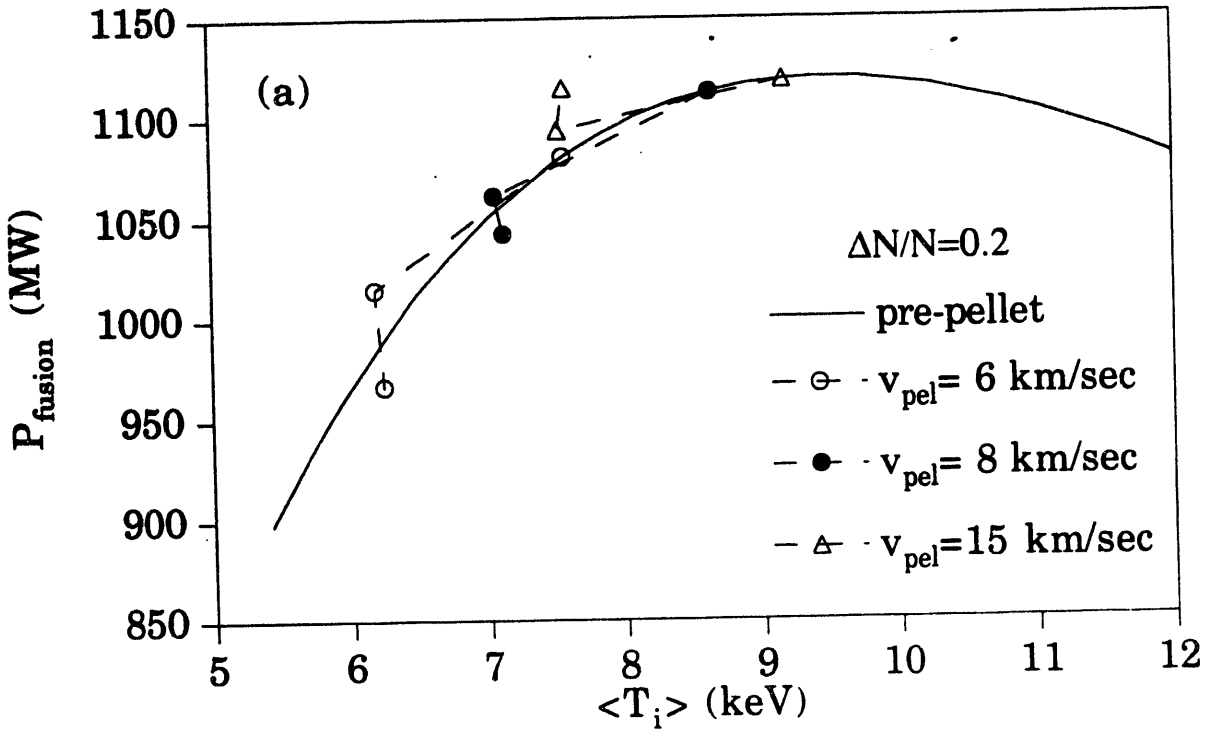
(a)
ΔN/N=0.2
pre-pellet
v_pel= 6 km/sec
v_pel= 8 km/sec
v_pel=15 km/sec
P_fusion (MW)
<T_i> (keV)
1150
1100
1050
1000
950
900
850
5
6
7
8
9
10
11
12

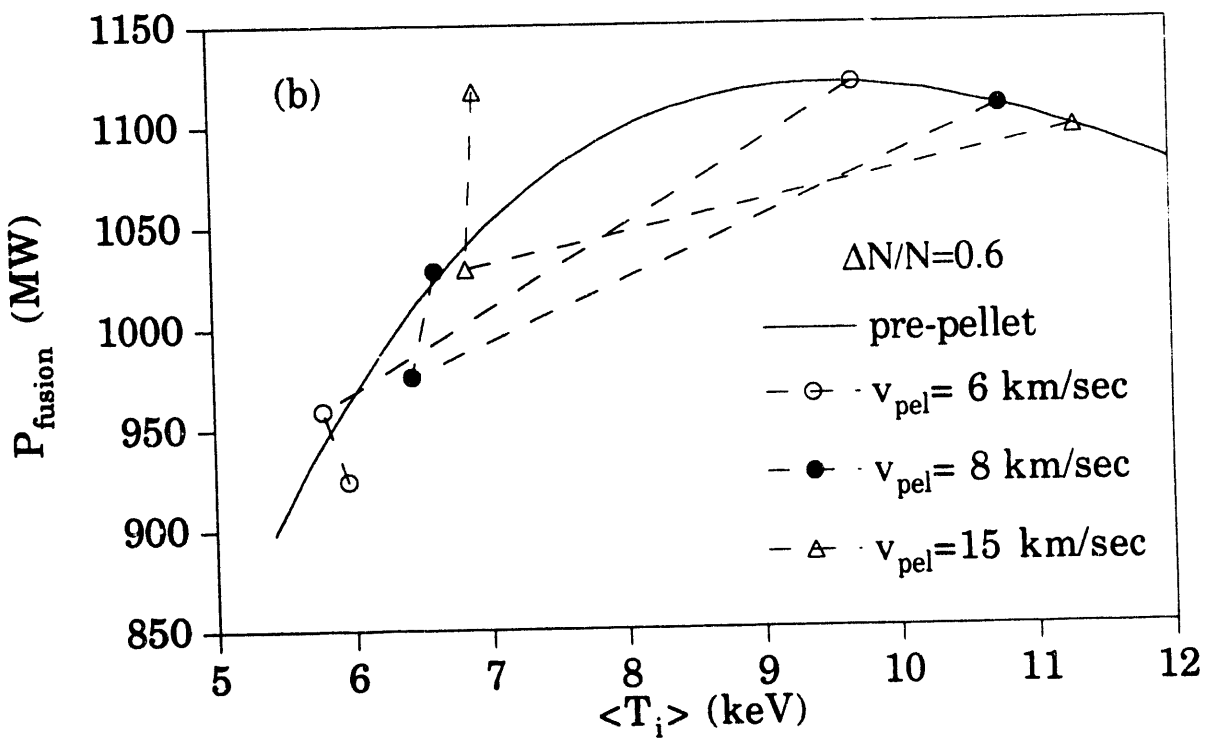
(b)
ΔN/N=0.6
pre-pellet
v_pel= 6 km/sec
v_pel= 8 km/sec
v_pel=15 km/sec
P_fusion (MW)
<T_i> (keV)
1150
1100
1050
1000
950
900
850
5
6
7
8
9
10
11
12

Figure 7

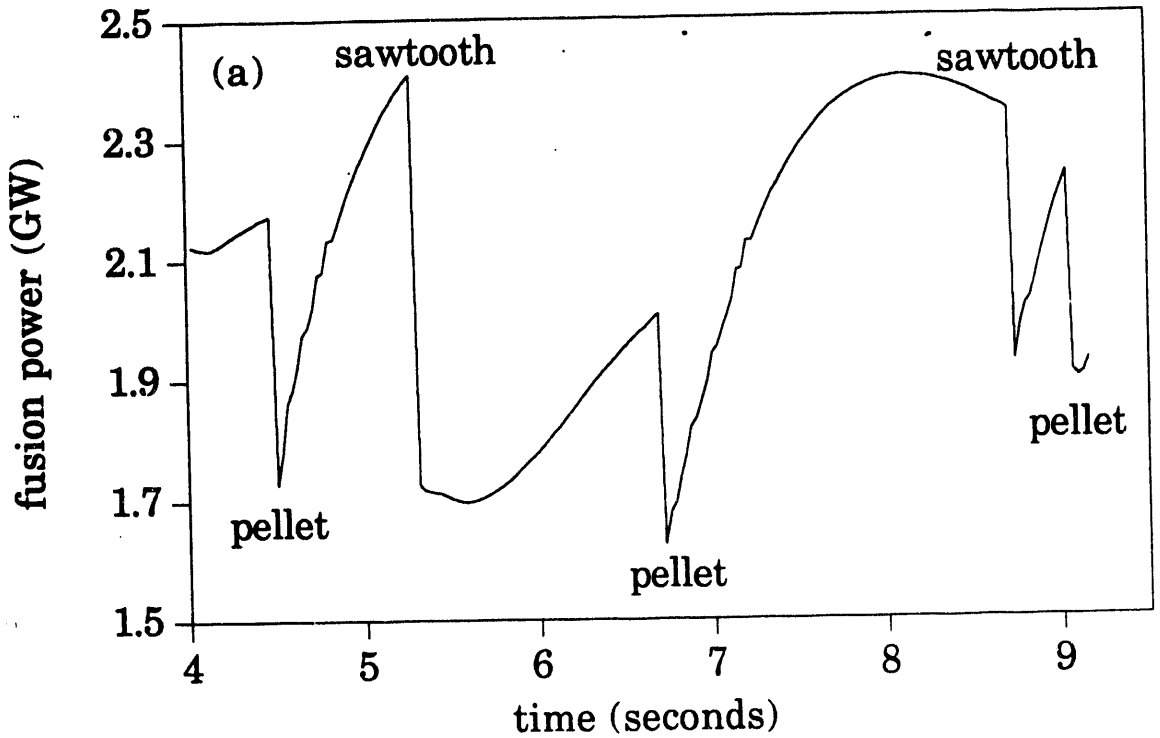
(a)
sawtooth
sawtooth
pellet
pellet
pellet
fusion power (GW)
2.5
2.3
2.1
1.9
1.7
1.5
4
5
6
7
8
9
time (seconds)

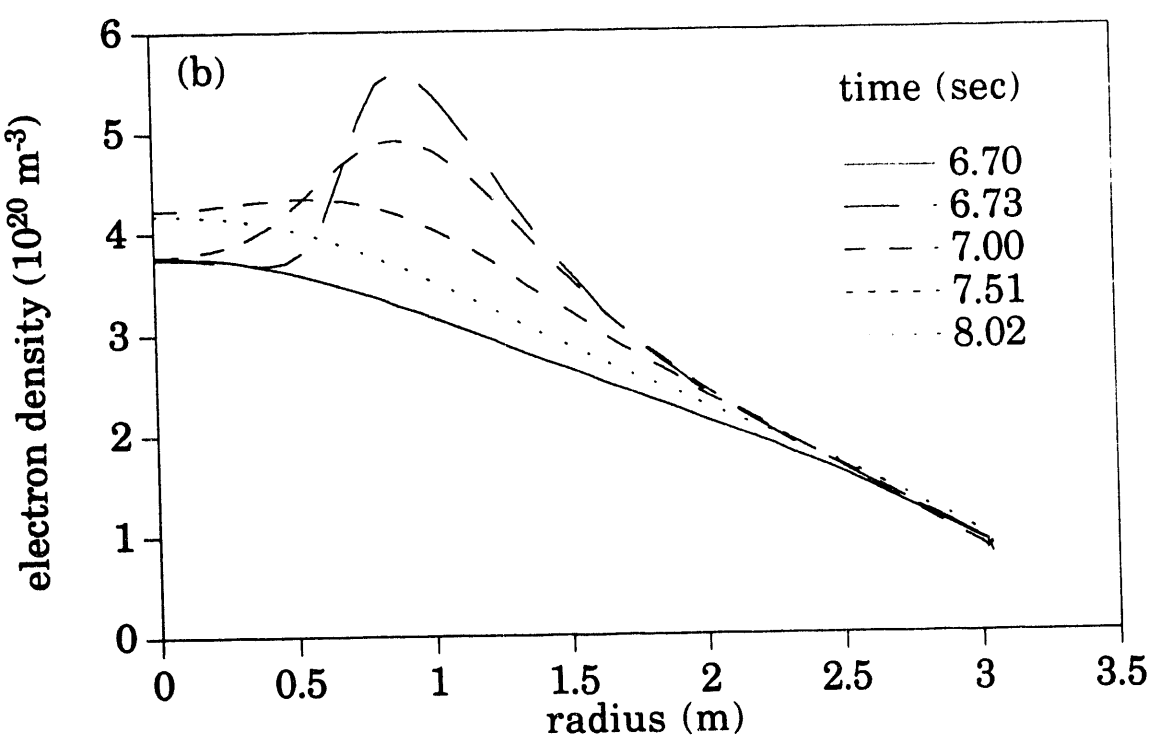
(b)
time (sec)
6.70
6.73
7.00
7.51
8.02
electron density (10^{20} m^{-3})
6
5
4
3
2
1
0
0
0.5
1
1.5
2
2.5
3
3.5
radius (m)

Figure 8

EXTERNAL DISTRIBUTION IN ADDITION TO UC-420

Dr. F. Paoloni, Univ. of Wollongong, AUSTRALIA
Prof. R.C. Cross, Univ. of Sydney, AUSTRALIA
Plasma Research Lab., Australian Nat. Univ., AUSTRALIA
Prof. I.R. Jones, Flinders Univ, AUSTRALIA
Prof. F. Cap, Inst. for Theoretical Physics, AUSTRIA
Prof. M. Heindler, Institut für Theoretische Physik, AUSTRIA
Prof. M. Goossens, Astronomisch Instituut, BELGIUM
Ecole Royale Militaire, Lab. de Phy. Plasmas, BELGIUM
Commission-European, DG. XII-Fusion Prog., BELGIUM
Prof. R. Boucique, Rijksuniversiteit Gent, BELGIUM
Dr. P.H. Sakanaka, Instituto Fisica, BRAZIL
Prof. Dr. I.C. Nascimento, Instituto Fisica, Sao Paulo, BRAZIL
Instituto Nacional De Pesquisas Espaciais-INPE, BRAZIL
Documents Office, Atomic Energy of Canada Ltd., CANADA
Ms. M. Morin, CCFM/Tokamak de Varennes, CANADA
Dr. M.P. Bachynski, MPB Technologies, Inc., CANADA
Dr. H.M. Skarsgard, Univ. of Saskatchewan, CANADA
Prof. J. Teichmann, Univ. of Montreal, CANADA
Prof. S.R. Sreenivasan, Univ. of Calgary, CANADA
Prof. R. Marchand, INRS-Energie et Materiaux, CANADA
Dr. R. Bolton, Centre canadien de fusion magnétique, CANADA
Dr. C.R. James,, Univ. of Alberta, CANADA
Dr. P. Lukác, Komenského Universzita, CZECHO-SLOVAKIA
The Librarian, Culham Laboratory, ENGLAND
Library, R61, Rutherford Appleton Laboratory, ENGLAND
Mrs. S.A. Hutchinson, JET Library, ENGLAND
Dr. S.C. Sharma, Univ. of South Pacific, FIJI ISLANDS
P. Mähönen, Univ. of Helsinki, FINLAND
Prof. M.N. Bussac, Ecole Polytechnique,, FRANCE
C. Mouttet, Lab. de Physique des Milieux Ionisés, FRANCE
J. Radet, CEN/CADARACHE - Bat 506, FRANCE
Prof. E. Economou, Univ. of Crete, GREECE
Ms. C. Rinni, Univ. of Ioannina, GREECE
Preprint Library, Hungarian Academy of Sci., HUNGARY
Dr. B. DasGupta, Saha Inst. of Nuclear Physics, INDIA
Dr. P. Kaw, Inst. for Plasma Research, INDIA
Dr. P. Rosenau, Israel Inst. of Technology, ISRAEL
Librarian, International Center for Theo Physics, ITALY
Miss C. De Palo, Associazione EURATOM-ENEA , ITALY
Dr. G. Grosso, Istituto di Fisica del Plasma, ITALY
Prof. G. Rostangni, Istituto Gas Ionizzati Del Cnr, ITALY
Dr. H. Yamato, Toshiba Res & Devel Center, JAPAN
Prof. I. Kawakami, Hiroshima Univ., JAPAN
Prof. K. Nishikawa, Hiroshima Univ., JAPAN
Librarian, Naka Fusion Research Establishment, JAERI, JAPAN
Director, Japan Atomic Energy Research Inst., JAPAN
Prof. S. Itoh, Kyushu Univ., JAPAN
Research Info. Ctr., National Instit. for Fusion Science, JAPAN
Prof. S. Tanaka, Kyoto Univ., JAPAN
Library, Kyoto Univ., JAPAN
Prof. N. Inoue, Univ. of Tokyo, JAPAN
Secretary, Plasma Section, Electrotechnical Lab., JAPAN
Dr. O. Mitarai, Kumamoto Inst. of Technology, JAPAN
Dr. G.S. Lee, Korea Basic Sci. Ctr., KOREA
J. Hyeon-Sook, Korea Atomic Energy Research Inst., KOREA
D.I. Choi, The Korea Adv. Inst. of Sci. & Tech., KOREA
Prof. B.S. Liley, Univ. of Waikato, NEW ZEALAND
Inst of Physics, Chinese Acad Sci PEOPLE'S REP. OF CHINA
Library, Inst. of Plasma Physics, PEOPLE'S REP. OF CHINA
Tsinghua Univ. Library, PEOPLE'S REPUBLIC OF CHINA
Z. Li, S.W. Inst Physics, PEOPLE'S REPUBLIC OF CHINA
Prof. J.A.C. Cabral, Instituto Superior Tecnico, PORTUGAL
Prof. M.A. Hellberg, Univ. of Natal, S. AFRICA
Prof. D.E. Kim, Pohang Inst. of Sci. & Tech., SO. KOREA
Prof. C.I.E.M.A.T, Fusion Division Library, SPAIN
Dr. L. Stenflo, Univ. of UMEA, SWEDEN
Library, Royal Inst. of Technology, SWEDEN
Prof. H. Wilhelmson, Chalmers Univ. of Tech., SWEDEN
Centre Phys. Des Plasmas, Ecole Polytech, SWITZERLAND
Bibliotheek, Inst. Voor Plasma-Fysica, THE NETHERLANDS
Asst. Prof. Dr. S. Cakir, Middle East Tech. Univ., TURKEY
Dr. V.A. Glukhikh,Sci. Res. Inst. Electrophys.I Apparatus, USSR
Dr. D.D. Ryutov, Siberian Branch of Academy of Sci., USSR
Dr. G.A. Eliseev, I.V. Kurchatov Inst., USSR
Librarian, The Ukr.SSR Academy of Sciences, USSR
Dr. L.M. Kovrizhnykh, Inst. of General Physics, USSR
Kernforschungsanlage GmbH, Zentralbibliothek, W. GERMANY
Bibliothek, Inst. Für Plasmaforschung, W. GERMANY
Prof. K. Schindler, Ruhr-Universität Bochum, W. GERMANY
Dr. F. Wagner, (ASDEX), Max-Planck-Institut, W. GERMANY
Librarian, Max-Planck-Institut, W. GERMANY

DATE
FILMED
7/29/94

END